Int J Clin Exp Pathol 2018;11(3):1575-1580
www.ijcep.com /ISSN:1936-2625/IJCEP0070713

Original Article

Influence of SIRT6 regulation of cellular glycometabolism on radiosensitivity of non-small-cell lung cancer A549 cells

Yong Cai[1], Zhaoying Sheng[1], Yun Chen[1], Jiying Wang[2]

Departments of [1]Radiation Oncology, [2]Oncology, Shanghai Pulmonary Hospital, Tongji University School of Medicine, Shanghai, China

Received December 10, 2017; Accepted December 28, 2017; Epub March 1, 2018; Published March 15, 2018

Abstract: Objective: To investigate the influence of SIRT6 mediated regulation of cellular glycometabolism on radiosensitivity of A549 non-small-cell lung cancer (NSCLC) cells. Methods: Ad-SIRT6 adenovirus vector overexpressed SIRT6 and was established and divided into a control group, a zero-load group (Ad-null), and an overexpression group (Ad-SIRT6). The virus concentration of the Ad-null group and the Ad-SIRT6 group was 200 pfu/cell. The survival factor (SF) after X-ray irradiation of 0, 2, 4, 6, 8, and 10 Gy in three groups was detected by clone formation and cell cycle and apoptosis after 4 Gy X-ray irradiation for 48 hours in the three groups was detected by flow cytometry. Expression levels of pyruvate kinase (PKM), lactate dehydrogenase (LDHA), and hexokinase (HK) after 4 Gy X-ray irradiation of 48 h were detected by qPCR. The glucose level after consumption of (1×10^6) cells in the medium was detected by a glucose kit. Results: Compared with the control group and the Ad-null group, SFs after X-ray irradiation of 4-10 Gy in the Ad-SIRT6 group were decreased ($P<0.05$). A sensitization enhancement ratio of the Ad-SIRT group/the control group was 1.451. After 4 Gy X-ray irradiation of 48 h, the cell ratio and apoptosis rate in G_1 phase were increased in the Ad-SIRT6 group, with statistical significance when compared with the other two groups ($P<0.05$). Compared with the control group and the Ad-null group, levels of PKM, LDHA, and HK mRNA in Ad-SIRT6 group were decreased ($P<0.05$) and the remaining glucose in the medium was increased ($P<0.05$). Conclusion: Overexpression of SIRT6 can inhibit key-enzyme generation in A549 cells to inhibit glycolysis, enhance the radiosensitivity, and lead to G_0/G_1 phase block as well as cell apoptosis.

Keywords: SIRT6, non-small-cell lung cancer, radiosensitivity, glycolysis

Introduction

Currently, the lung cancer is a widespread malignant tumor with the highest morbidity and mortality in the world, causing annual death up to 1.2 million people [1]. Non-small cell lung cancer comprises about 80%-85% in the lung cancer [2], while non-operable and local advanced-stage NSCLC takes about 40% [3]. The radio-therapeutic effect of NSCLC is dose-dependent. The high dose of radiotherapy can improve remission and control rates, but it will cause severe side effects like serious radioactive esophagitis and pneumonia [4]. Radioresistance of tumor tissue limits its clinical applications and the cure rate of malignant tumors [5]. The main cause for the radio-therapeutic failure is solid tumor hypoxia. Therefore, how to overcome that is a vital avenue to improve the effectiveness for treating tumor [6]. In recent years, many studies have brought out many ways to overcome the radioresistance caused by tumor hypoxia. Glycometabolism changes are frequent manifestations for metabolic reprogramming of tumor cells. Tumor cells can instantly accumulate glycolysis intermediates after the glycometabolism switching to aerobic glycolysis, laying a foundation to cell growth and macromolecular synthesis for proliferation. SIRT6, a part of NAD+-dependent histone deacetylase, regulates and controls physiological processes like the cell growth and apoptosis [7]. Some studies have found that the severe metabolic disorder, lethal hypoglycemia and excessive glucose intake of muscle and fat under the normal condition may occur in SIRT6 flaw mice [7]. The role and the mechanism of SIRT6 regulating and controlling energy

Table 1. Relavent PCR primer sequences

Name	Primer Sequence
PKM	Forward primer 5'-GCT AAG GCA CGC GGT G-3'
PKM	Reverse primer 5'-GTG CAG GGT CCG AGG T-3'
LDHA	Forward primer 5'-CTC GCT TCG GCA GCA CAT ATA CT-3'
LDHA	Reverse prime 5'-ACG CTT CAC GAA TTT GCG TGT C-3'
HK	Forward primer 5'-GAA GGA CAT CAG CGG TAA GA-3'
HK	Reverse prime 5'-AGA TAG ACC AGT GGA GAC AC-3'
GAPDH	Forward primer 5'-GGA GTC CAC TGG CGT CTT-3'
GAPDH	Reverse prime 5'-GAG TCC TTC CAC GAT ACC AA-3'

Table 2. Parameter values for multi-target click model fit in clone formation

Group	D_0 (Gy)	D_q (Gy)	SF_2	SER
Control Group	1.542	1.970	0.685	
Ad-SIRT6 Group	1.062	1.605	0.527	1.451
Ad-null Group	1.600	2.013	0.730	0.958

metabolism in tumor radioresistance was the focus of this research. We discovered that the influence of SIRT6 is in regulating and controlling glycometablism in A549 radio-resistance of NSCLC cells. This research is sponsored by the Shanghai Natural Science Foundation of China (15ZR1434300).

Materials and methods

Cells, materials and reagents

A549 cells were purchased from the cell bank of the Shanghai Institute of Organic Chemistry, Chinese Academy of Science. RPMI-1640 nutrient medium and fetal bovine serum were purchased from American Gibico company. PBS was purchased from Solarbio company. Vector construction of SIRT6 over-expressive adenovirus vector was established by Shanghai Genechem Co.,Ltd. Lipofectamine™ 2000 and Trizol were purchased from American Invitrogen Company. PrimeScript™ RT-PCR kit and SYBR® PremixExTaq™II kit were purchased from Japanese TaKaRa company. Trypsinase, CCK-8 cell proliferation assay kit, Annexin V-FITC apoptosis assay kit, Hoechst 33258 staining kit and crystal violet dye were purchased from Beyotime Biotechnology Company. Western blot experiment-related reagents were purchased from Beyotime Biotechnology Company. Primers of PKM, LDHA, and HK were purchased from Shanghai Sangon Biotech Company.

Cell culture, transfection and irradiation requirement

RPMI-1640 medium (containing 10% fetal bovine serum) was used to culture cell and placed in the 37°C and 5% CO_2 cell incubator. When cell fusion reached about 85%, the cells were sub-cultured via trypsin digestion. A549 cells in logarithmic phase were spread in the six-well plate with a density of 4×10^5/well after dissociation and resuspension. When adherent, the zero load (Ad-null group) and lentivirus overexpressing SIRT6 (Ad-SIRT6 group) were transfected into A549 cells, with a virus concentration of 200 pfu/cell. After transfection of 6 h, the medium was replaced as complete medium and the transfection efficiency was observed with fluorescence microscope. The irradiation condition of 6 MVX ray was hand-rotated 180°, vertically irradiating the cells from bottom to up. Vaseline of 1 cm was matted under the cultivation plate and source-skin distance was 100 cm.

RT-PCR to detect expression levels of PKM, LDHA, and HK mRNA

After transfection for 48 h, total RNA was extracted according to the Trizol reagent directions and cDNA was synthesized by PrimeScript™ RT-PCR reagent kit directions. According to the SYBR® PremixExTaqTM (TliRNaseHPlus) reagent kit directions, fluorescent quantitating PCR via ABI 7500 real-time PCR meter to detect the expression level of PKM, LDHA, and HK mRNA. GAPDH was taken as reference gene. The $2^{-\Delta\Delta ct}$ method was used to calculate the relative expression of PKM, LDHA, and HK mRNA. There were 3 lateral apertures in each experimental group. **Table 1** shows relative PCR primers.

Flow cytometry to analyze the mitotic cycle

After transfection of 48 h, the trypsinized, resuspended, and centrifugated A549 cells were rinsed by pre-chilled PBS and fixed in the 75% ethanol overnight at 4°C. The cells were then rinsed by the pre-chilled PBS, dyed by propidium iodide staining, and incubated 30 min under 37°C and away from light. There were at least 3 lateral apertures in each group. The cell cycle distribution was detected by BD FACSCanto™ flow cytometer.

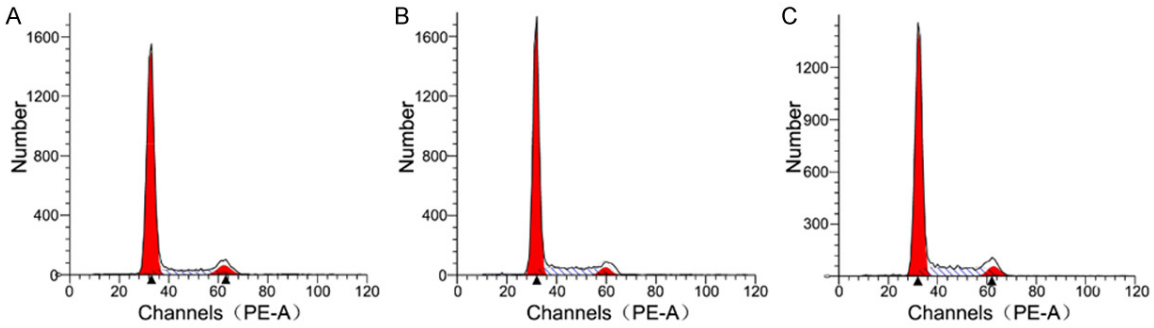

Figure 1. A549 cell cycle in different groups detected by flow cytometer. A: Ad-SIRT6 Group; B: Control Group; C: Ad-null Group.

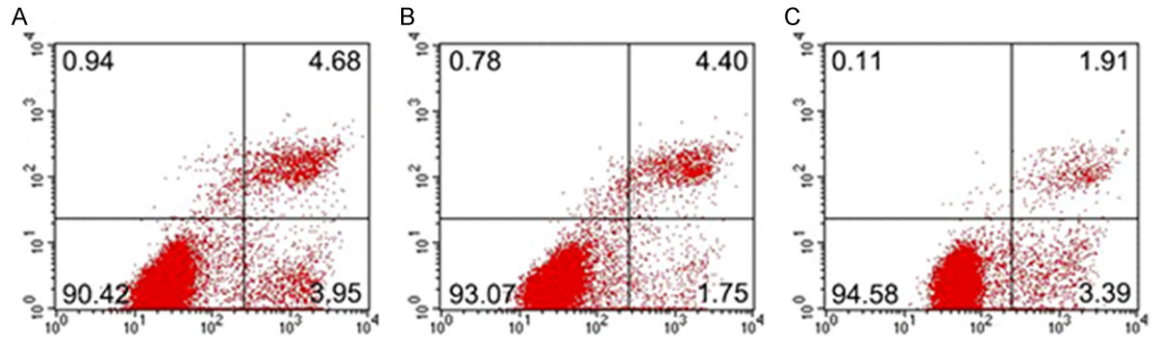

Figure 2. A549 cell apoptosis rate in different transfection groups after non-irradiation and 8 Gy irradiation detected by flow cytometry. A: Ad-SIRT6 Group; B: Control Group; C: Ad-null Group.

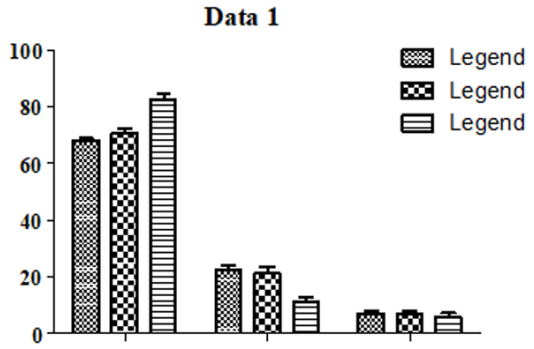

Figure 3. PI single staining flow cytometry cell cycle analysis of different transfected cells. The results showed that there was no significant difference in the cell cycle distribution between the control group and the ADNULL group (P>0.05). Compared with the other two groups, the proportion of cells in the G_0/G_1 phase in the ADSIRT6 group at 48 hours after 4 Gy X-ray irradiation increased, S phase cells decreased, the difference was statistically significant (P<0.05).

Annexin V/PI dual staining to detect cell apoptosis

After transfection for 24 h, the cells were irradiated by 6 MVX of 8 Gy ad cultured in the incubator for 48 h. The control group without irradiation was set. After cell dissociation and resuspension (the origin culture solution was kept), the cell count was about 80,000. After centrifugation, the Annexin V-FITC mixture was added; then fully resuspended. The Annexin V-FITC was added again to fully mix and the propidium iodide staining was added and mixed to cultivate 20 min without light in room temperature. BD FACSCanto™ flow cytometer was used to detect the apoptosis rate in the early and late stage.

Clone formation

After infection for 24 h, the cells were trypsinized, resuspended, and counted. The cells were placed in 6-well plates in accordance with different 6MVX ray doses of 0 Gy, 2 Gy, 4 Gy, 6 Gy, 8 Gy, and 10 Gy and different densities of 200, 500, 1000, 3000, and 5000 cells/well. At least 3 lateral apertures were established at each dose position. When adherence occurred, the cells were irradiated and cultivated for another 1-2 weeks. When macroscopic cell colony could be seen in the 6-well plate, the cells were rinsed by PBS twice and fixed in ethanol

Table 3. Comparison of the cellular cycle ratio among three groups (±s)

Group	Cell cycle ratio (%)		
	G_0/G_1 Phase	S Phase	G_2/M Phase
Ad-SIRT6 Group	82.49±1.97	11.87±1.38	5.64±0.72
Control Group	74.58±1.28	19.88±0.26	5.54±1.05
Ad-null Group	68.19±3.30	24.84±2.11	6.97±1.25

Table 4. Cell apoptosis rate in different groups detected by flow cytometry

Group	Non-irradiation	8 Gy irradiation
Ad-SIRT6 group	8.18±0.42	33.40±2.02
Control Group	6.31±0.60	19.61±1.47
Ad-null Group	5.68±0.33	12.28±0.70

Table 5. Influence of SIRT6 over-expression on enzyme level of A549 glycolysis

Group	PKM	LDHA	HK
Control Group	1.102±0.213	1.064±0.035	1.133±0.212
Ad-null Group	0.944±0.194	0.984±0.121	1.028±0.197
Ad-SIRT6 Group	0.544±0.186	0.148±0.114	0.662±0.094

for 15 min. The cells were then rinsed again by PBS for twice and dyed for 20 min with 0.1% crystal violet. Numbers of the monoclonal colony ≥50 were counted microscopically and the cell survival rate in each group was calculated. Siha cell survival curve was established by GraphPadPrime 5.0 software and the multi-target click model fit was designed through analysis to calculate the relative radiation biological parameters.

Glucose level in the medium

After transfection for 24 h, the cells were trypsinized, resuspended, and counted. The cells were placed in a 96-well plate with 2000 cells/well and at least 3 lateral apertures were established at each dose position. After adherence for 72 h, the glucose kit reagent was added and incubated 3 h under 37°C. ELISA was used to detect the absorbance OD value in the A450 nm according to kit.

Statistical analysis

The SPSS Statistics 23 software was used to analyze the experimental data and a t test method was used to analyze the expressive difference among clinical tissue specimen. Repeated measurement data variance analysis and the independent sample t test method or factor analysis of variance was used to compare other data. P<0.05 means that the difference has statistical significance.

Results

The influence of overexpression of SIRT6 on A549 cell radio-sensitivity

Clone formation showed that after irradiation of different 6MVX dose, SF decreased significantly, with a sensitization enhancement ratio that was higher in A549 cells over-expressing SIRT6, while the transfected AD-null had no influence on those indexes. These data indicate that after Ad-SIRT6 transfection, the radio-sensitivity of A549 cells increased. **Table 2** shows relative radiation parameters.

The influence of SIRT6 overexpression on A549 mitotic cycle

The flow cytometer was used to detect the mitotic cycle in different transfected group. **Figure 3** shows in detail. G_1 phase in the Ad-SIRT6 group was significantly higher than that in the control group, ratio of S phase was lower than that in the group (P=0.004; P=0.001). The ratio of G_1 and S phase in the Ad-null group had no statistically significant difference (P>0.05). The G2/M cell ratio in the three groups had no statistically significant difference (F=1.797, P=0.2450). This is shown in detail in **Figure 1** and **Table 3**.

The influence of SIRT6 overexpression on A549 cell apoptosis

Ad-SIRT6 and Ad-null were transfected into A549 cells and the flow cytometer was used to detect the apoptosis. **Table 4** shows in detail. Without X-ray irradiation, the apoptosis rate in the Ad-SIRT6 group was higher than that in the control group, while that in the Ad-null group had no significant difference (*P*=0.03; *P*=0.145); while after 4 Gy X-ray irradiation, the apoptosis rate in the Ad-SIRT6 group was sig-

Table 6. Cell multiplication OD value of A549 in different groups with different cultivating time (±s)

Group	Glucose Level (OD Value)				
	0 h	12 h	24 h	48 h	72 h
Ad-null Group	0.378±0.019	0.598±0.062	0.674±0.015	0.882±0.048	1.466±0.059
Control Group	0.403±0.007	0.732±0.007	0.770±0.017	1.190±0.026	2.237±0.223
Ad-SIRT6 Group	0.376±0.008	0.714±0.029	0.833±0.012	1.653±0.099	3.129±0.105

nificantly increased than that in the control group ($P<0.001$), suggesting that the Ad-SIRT6 overexpressing SIRT6 can improve the radiosensitivity of A549 cells by advancing the apoptosis. **Figure 2** shows this data in detail.

The influence of SIRT6 on enzyme level in the process of A549 glycolysis

Compared with the control group and the Ad-null group, the level of PKM, LDHA, and HK mRNA in the Ad-SIRT6 group was decreased ($P<0.05$). The level of PKM, LDHA, and HK mRNA in the control group and Ad-null group had no statistically significant difference ($P>0.05$). **Table 5** shows this in detail.

The influence of SIRT6 overexpression on glucose level in the medium

The OD value of A549 was detected to evaluate the cell proliferation ability. **Table 6** shows this in detail. According to the variance analysis of repeated measurement data, the OD value in the Ad-SIRT6 group was increased when compared with the control group ($P<0.001$), showing that the overexpressing Ad-SIRT6 vector can inhibit the absorption of glucose.

Discussion

Radioresistance is the main cause to restrict tumor radio-therapeutic effects and lead to radio-therapeutic failure. The mechanism of radiotherapy is to induce apoptosis of tumor cells and irreversible cell cycle arrest by damaging the DNA of tumor cells. Glycometabolism changes are frequent manifestations for metabolic reprogramming of tumor cells. Tumor cells can immediately accumulate glycolytic intermediates after glycometabolism switching to aerobic glycolysis, laying a foundation to the cell growth and macromolecular synthesis for proliferation [11]. Although the majority of tumor cells can up-regulate glucose transporter to absorb more glucose [12, 13], the tumor cell also can further improve the glycometabolism and lactic acid production rate by up-regulating the level and activity of some glycolytic enzymes (such as phosphofructokinase-1, pyruvate kinase M2, LDHA, and pyruvate dehydrogenase kinase-1) [14]. Many studies have suggested that down-regulating the LDHA or pyruvate dehydrogenase kinase-1 can inhibit the tumor cell growth and slow down the proliferation rate [15-17], showing that the rate-limiting enzyme plays a vital role in the metabolic reprogramming which is essential to the growth and proliferation of tumor cells. Glycolysis in tumor cells is 200 times higher than in normal cells. Lacking SIRT6 may significantly enhance the glycolysis rate of tumor cells. The skin cell from SIRT6-deficient embryo mice was cultivated in vitro, with a high proliferation rate and it transformed immediately when injected into the adult mice, showing the oncogenicity of the SIRT6 gene. But whether the SIRT6 is related to the activation of cancer cells is not known, showing that SIRT6 can be regarded as an anti-oncogene which can influence the proliferation of tumor cells by regulating the tumor metabolism. SIRT6 protein can also inhibit tumorigenesis because SIRT6 can inhibit the hypermetabolism activity. SIRT6 is not a classic metabolic zymoprotein, but a modulin in charge of gene integrity and ensuring expression of genome. SIRT6 protein can inhibit the transformation of cells and can prevent further development of tumor cells, because SIRT6 protein can inhibit the metabolic activity. More accurately, SIRT protein can inhibit glycolysis and protein synthesis.

This study found that SIRT6 overexpression decreased the survival ability of A549 cells and resulted in a sensitization enhancement rate that was increased to 1.451 when compared with the control group. Therefore, SIRT6 overexpression can enhance the radio-sensitivity of A549 cells and effectively reduce radioresistance of NSCLC cells. Besides inhibiting the A549 cells' proliferation, this research also

found that cell ratio and apoptosis rate in G_1 phase of A549 cell were increased, showing that SIRT6 can lead to G_0/G_1 inhibition and apoptosis. Levels of PKM, LDHA, and HK mRNA after the SIRT6 overexpression were decreased ($P<0.05$) and levels of glucose in the medium was increased ($P>0.05$). In summary, overexpression of SIRT6 can inhibit key-enzyme generation in A549 cells to inhibit glycolysis, enhance radio-sensitivity, and lead to G_0/G_1 phase block as well as induce cell apoptosis.

Acknowledgements

This study was supported by Shanghai Natural Science Foundation of China (15ZR1434300).

Disclosure of conflict of interest

None.

Address correspondence to: Jiying Wang, Depart ment of Oncology, Shanghai Pulmonary Hospital, Tongji University School of Medicine, Shanghai 200433, China. Tel: 86-21-65115006; E-mail: wangjiying_1@yeah.net

References

[1] Chen W, Zheng R, Baade PD, Zhang S, Zeng H, Bray F, Jemal A, Yu XQ, He J. Cancer statistics in China, 2015. CA Cancer J Clin 2016; 66: 115-132.

[2] Vordermark D. Radiotherapy of cervical cancer. Oncol Res Treat 2016; 39: 516-520.

[3] Barker HE, Paget JT, Khan AA, Harrington KJ. The tumour microenvironment after radiotherapy: mechanisms of resistance and recurrence. Nat Rev Cancer 2015; 15: 409-425.

[4] Taguchi YH. Identification of more feasible MicroRNA-mRNA interactions within multiple cancers using principal component analysis based unsupervised feature extraction. Int J Mol Sci 2016; 17.

[5] Gonzalez-Quintana V, Palma-Berre L, Campos-Parra AD, López-Urrutia E, Peralta-Zaragoza O, Vazquez-Romo R, Pérez-Plasencia C. MicroRNAs are involved in cervical cancer development, progression, clinical outcome and improvement treatment response (Review). Oncol Rep 2016; 35: 3-12.

[6] Wang QQ, Wang MJ, Zhang YH, et al. Effects of miR-449a on proliferation, migration and invasion of esophageal squamous-cell carcinoma cell line Eca-109. Shandong Medical Journal 2017; 1042: 24-27.

[7] Zhao Y, Ling Z, Hao Y, Pang X, Han X, Califano JA, Shan L, Gu X. MiR-124 acts as a tumor suppressor by inhibiting the expression of sphingosine kinase 1 and its downstream signaling in head and neck squamous cell carcinoma. Oncotarget 2017; 8: 25005-25020.

[8] He Y, Zhao C, Liu Y, He Z, Zhang Z, Gao Y, Jiang J. Reracted article: miR-124 functions as a tumor suppressor via targeting hCLOCK1 in glioblastoma. Mol Neurobiol 2017; 54: 2375.

[9] Li W, Huang H, Su J, Ji X, Zhang X, Zhang Z, Wang H. miR-124 acts as a tumor suppressor in glioblastoma via the inhibition of signal transducer and activator of transcription 3. Mol Neurobiol 2017; 54: 2555-2561.

[10] Ma T, Zhao Y, Wei K, Yao G, Pan C, Liu B, Xia Y, He Z, Qi X, Li Z, Wang J, Shao Y. MicroRNA-124 functions as a tumor suppressor by regulating CDH2 and epithelial-mesenchymal transition in non-small cell lung cancer. Cell Physiol Biochem 2016; 38: 1563-1574.

[11] Wang Y, Chen L, Wu Z, Wang M, Jin F, Wang N, Hu X, Liu Z, Zhang CY, Zen K, Chen J, Liang H, Zhang Y, Chen X. miR-124-3p functions as a tumor suppressor in breast cancer by targeting CBL. BMC Cancer 2016; 16: 826.

[12] Wu Z, Huang W, Chen B, Bai PD, Wang XG, Xing JC. Up-regulation of miR-124 inhibits invasion and proliferation of prostate cancer cells through mediating JAK-STAT3 signaling pathway. Eur Rev Med Pharmacol Sci 2017; 21: 2338-2345.

[13] Zhang YH, Wang QQ, Li H, Ye T, Gao F, Liu YC. miR-124 radiosensitizes human esophageal cancer cell TE-1 by targeting CDK4. Genet Mol Res 2016; 15.

[14] Hao C, Xu X, Ma J, Xia J, Dai B, Liu L, Ma Y. MicroRNA-124 regulates the radiosensitivity of non-small cell lung cancer cells by targeting TXNRD1. Oncol Lett 2017; 13: 2071-2078.

[15] Zheng X, Han H, Liu GP, Ma YX, Pan RL, Sang LJ, Li RH, Yang LJ, Marks JR, Wang W, Lin A. LncRNA wires up Hippo and Hedgehog signaling to reprogramme glucose metabolism. EMBO J 2017; 36: 3325-3335.

[16] Tso SC, Lou M, Wu CY, Gui WJ, Chuang JL, Morlock LK, Williams NS, Wynn RM, Qi X, Chuang DT. Development of dihydroxyphenyl sulfonylisoindoline derivatives as liver-targeting pyruvate dehydrogenase kinase inhibitors. J Med Chem 2017; 60: 1142-1150.

[17] Takeda S, Okazaki H, Kudo T, Kakizoe K, Himeno T, Matsumoto K, Shindo M, Aramaki H. Bongkrekic acid as a warburg effect modulator in long-term estradiol-deprived MCF-7 breast cancer cells. Anticancer Res 2016; 36: 5171-5182.